Supporting Information

69451 Weinheim, Germany

Spontaneous α-C-H Carboxylation of Ketones by Gaseous CO_2 at the Air-water Interface of Aqueous Microdroplets

Pallab Basuri, Sinchan Mukhopadhyay, K. S. S. V. Prasad Reddy, Keerthana Unni, B. K. Spoorthi, Shantha Kumar Jenifer, S. R. K. C. Yamijala Sharma, and Thalappil Pradeep*

Abstract: We present a catalyst-free route for the reduction of carbon dioxide integrated with the formation of a carbon-carbon bond at the air/water interface of negatively charged aqueous microdroplets, at ambient temperature. The reactions proceed through carbanion generation at the α-carbon of a ketone followed by nucleophilic addition to CO_2. Online mass spectrometry reveals that the product is an α-ketoacid. Several factors, such as the concentration of the reagents, pressure of CO_2 gas, and distance traveled by the droplets, control the kinetics of the reaction. Theoretical calculations suggest that water in the microdroplets facilitates this unusual chemistry. Furthermore, such a microdroplet strategy has been extended to seven different ketones. This work demonstrates a green pathway for the reduction of CO_2 to useful carboxylated organic products.

DOI: 10.1002/anie.2021XXXXX

Table of Contents

Serial No.	Details	Page No
SI 1	Experimental details	3
Figure S1	MS/MS spectra of *m/z* 99 and 143	4
Scheme S1	Reaction scheme of water loss pathway and De-carboxylation pathway from the product *m/z* 143	5
Figure S2	Survival Yield calculation	6
Figure S3	Microdroplet carboxylation reaction with deuterated labeled AcAc.	7
Figure S4	Microdroplet carboxylation reaction showing absence of di-carboxylated product	8
SI 2	Bulk reaction and ESI MS measurements	9
Figure S5	Time-dependent ESI MS measurements of the bulk reaction mixtures	10
Figure S6	Background mass spectra were recorded using methanol and water	11
Figure S7	Effect of CO_2 gas pressure	12
Figure S8	Effect of total reagent concentration in the microdroplet carboxylation reaction	13
Figure S9	Spray voltage variation experiment	14
Figure S10	Microdroplet reaction mass spectrometry of reaction mixture containing 1:30 ratio of AcAc and $(NH_4)_2CO_3$.	15
Figure S11	Microdroplet reaction mass spectrometry between AcAc and CO_2 using ambient air nebulization	16
Figure S12	Positive ion mode microdroplet reaction mass spectrometry	17
Figure S13	Effect of a radical scavenger on the droplet carboxylation reaction	18
Figure S14	Distance experiments using AcAc and $(NH_4)_2CO_3$ reaction mixture	19
Figure S15	Distance experiments using AcAc and CO_2	20
Figure S16	Electrospray emitter tip diameter variation experiments	21
Figure S17	Microdroplet reaction by varying concentration of AcAc and $(NH_4)_2CO_3$	22
Figure S18	Dark field microscopic images of microdroplets	23
Figure S19	Solvent composition dependency of microdroplet reaction	24
Figure S20	Effect of pH on the reagent to product conversion ratio.	25
Figure S21	Effect of ionic strength on our microdroplet carboxylation reaction	26
SI 3	Details of DFT and coordinates for DFT calculation	27
Figure S22	Free energy landscape for Keto-enol transformation over AcAc	34
Figure S23	Free energy landscape for C-C bond formation in neutral and negatively charged microdroplets.	35
Figure S24	Microdroplet reaction with acetone and $(NH_4)_2CO_3$	36
Figure S25	Microdroplet reaction with of 1,1,1-trifluoro-5,5-dimethyl-2,4-hexanedione and $(NH_4)_2CO_3$	37
Figure S26	Microdroplet reaction with benzophenone and $(NH_4)_2CO_3$	38
Figure S27	Microdroplet reaction with acetophenone and $(NH_4)_2CO_3$	39
Figure S28	Microdroplet reaction with dimedone and $(NH_4)_2CO_3$	40
Figure S29	Microdroplet reaction with cyclopentane-1,3-dione and $(NH_4)_2CO_3$	41
Scheme S2	Scheme showing keto-enol tautomerism among a) AcAc, b) cyclopentane-1,3-dione, and c) 5,5-dimethyl-cyclohexane-1,3-dione, respectively	42
Figure S30	ESI MS spectrum of 2 h spray deposited sample after methanol extraction	43

Supporting Information 1:

Sampling and online mass spectrometric measurements:

We prepared 10 mM aqueous solutions for each of the reagents in Millipore water. The solutions were taken in a Hamilton 100 µL syringe and connected to a syringe pump to infuse (at 5 µL/min) through a fused silica capillary (ID = 100 µm; OD = 300 µm). The capillary and syringe were connected through a union connector. The flow rate of the sample was set to 5 µL/min. The high-voltage power supply was connected to the metallic needle of the syringe. Negative and positive 3-4 kV were applied to generate the charged microdroplets from the tip of the capillary. This home-built ESI setup was held in front of the mass spectrometer inlet at a distance of 1 cm (tip-to-inlet distance). Capillary and tube lens voltages were set to 2 and 20 V, respectively. The capillary temperature was set to 270 °C for most of the experiments. No nebulization gas was applied for most of the experiments. However, the gas pressure experiments were performed by connecting an N_2 source with the ESI source using a stainless-steel union T connector.

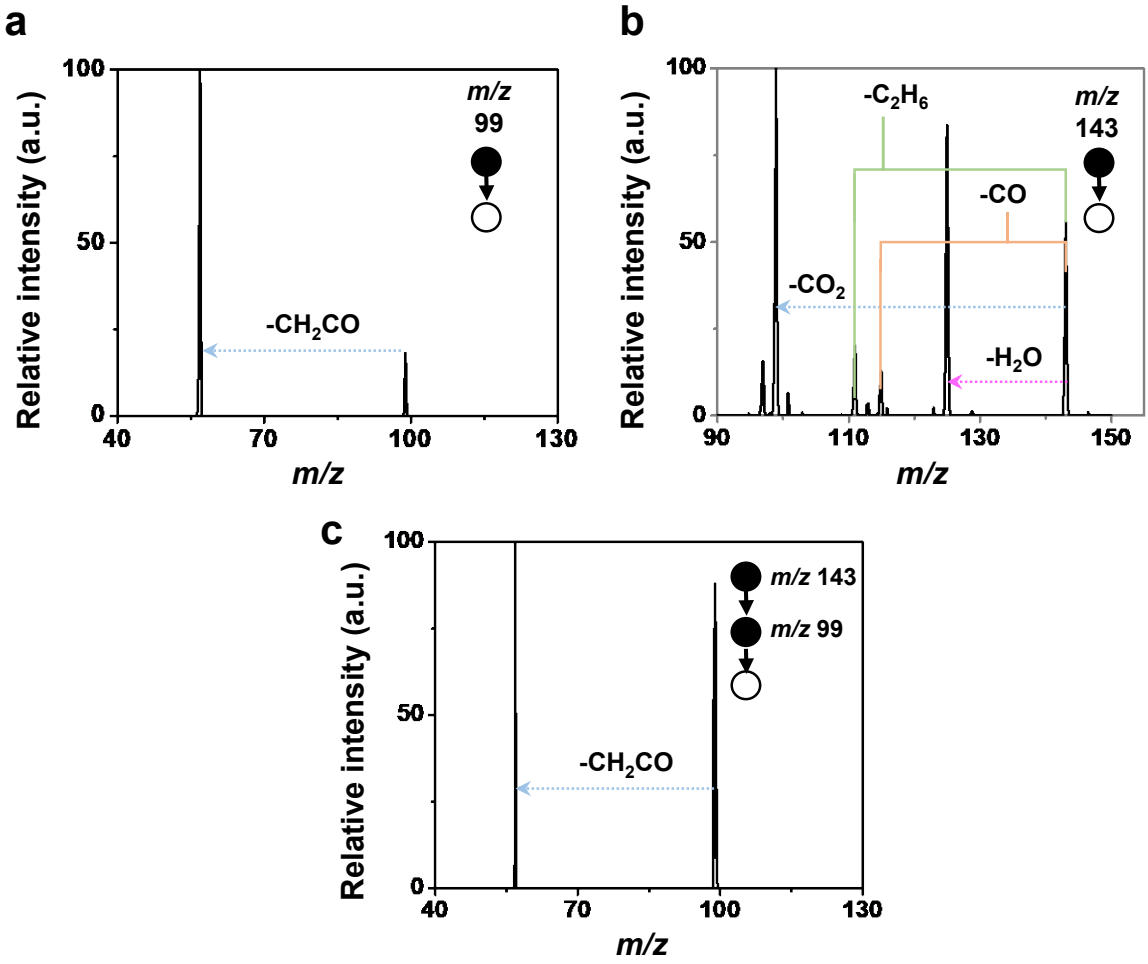

Figure S1. Collision-induced dissociation of the isolated peaks corresponding to the reagent and the product. a) MS/MS spectrum of *m/z* 99. b) MS/MS spectra of isolated ion of *m/z* 143 showing a major loss of 44 corresponding to CO_2. c) MS/MS/MS of the isolated product peak which further supports our assignment.

Water loss pathway

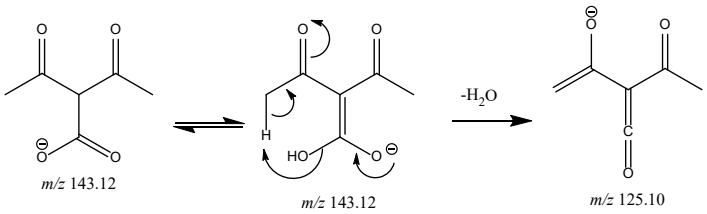

De-carboxylation pathway

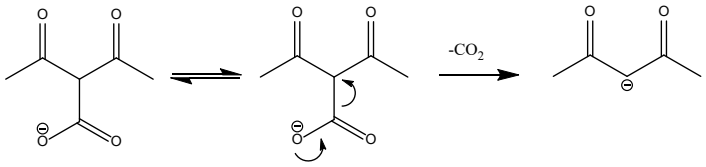

Scheme S1. Scheme showing neutral loss of a water and a CO_2 molecule from the isolated product peak during tandem mass spectrometry.

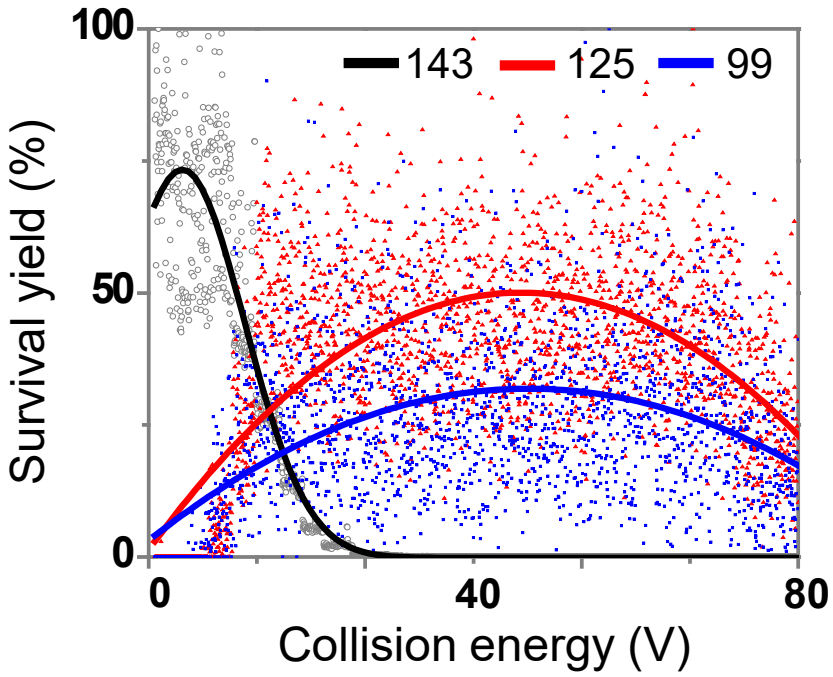

Figure S2. Survival yield plot of the reaction product under high collision energy showing that the C-C bond breaking that leads to a neutral loss of CO_2 from the parent ion takes 40 V collision energy.

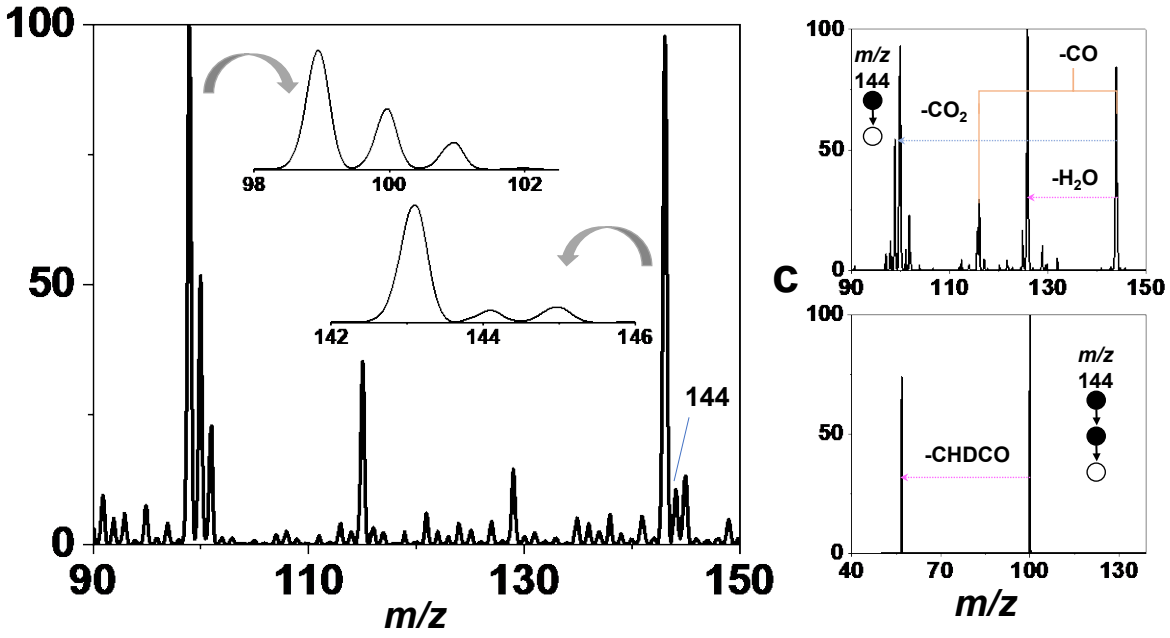

Figure S3. Microdroplet carboxylation of deuterated AcAc. a) Full range mass spectrum showing presence of mono-deuterated AcAc and product peak at *m/z* 100 and 144, respectively. b and c) MS/MS and MS/MS/MS of the isolated product peak. Peaks at *m/z* 121 and 131 correspond to background signal.

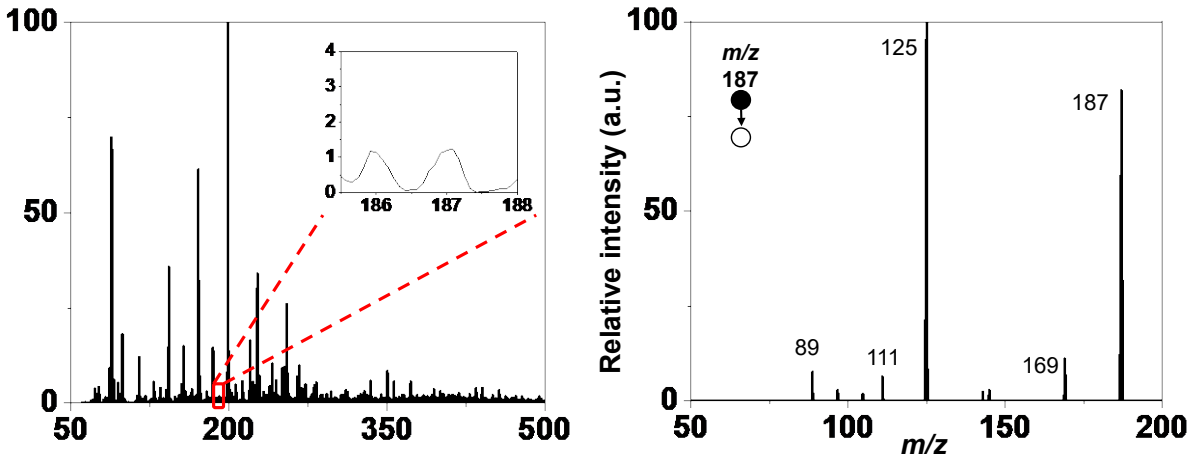

Figure S4. Microdroplet carboxylation reaction showing absence of di-carboxylated product. a) Full range mass spectrum showing absence of di-carboxylated product peak at *m/z* 187. Small signal in that position corresponds to a background signal which is further confirmed by the MS/MS of the peak (b), showing that the fragmentation pattern is not related to the product.

Supporting Information 2:

Bulk reaction and ESI MS measurements:

A bulk reaction was conducted by continuous bubbling of CO_2 gas from 1 minute up to 30 minutes in an aqueous solution containing 10 mM AcAc. A time-dependent ESI MS measurement was performed in a commercial ESI source with an LTQ-XL mass spectrometer to observe any product formation. We used N_2 as a nebulization gas and -3 kV as spray voltage. Mass spectra as a function of time are shown below where no peak at *m/z* 143 corresponding to product was observed. We only observed the reagent peak at *m/z* 99 as the base peak. All the other peaks at different time intervals are the result of the background signal.

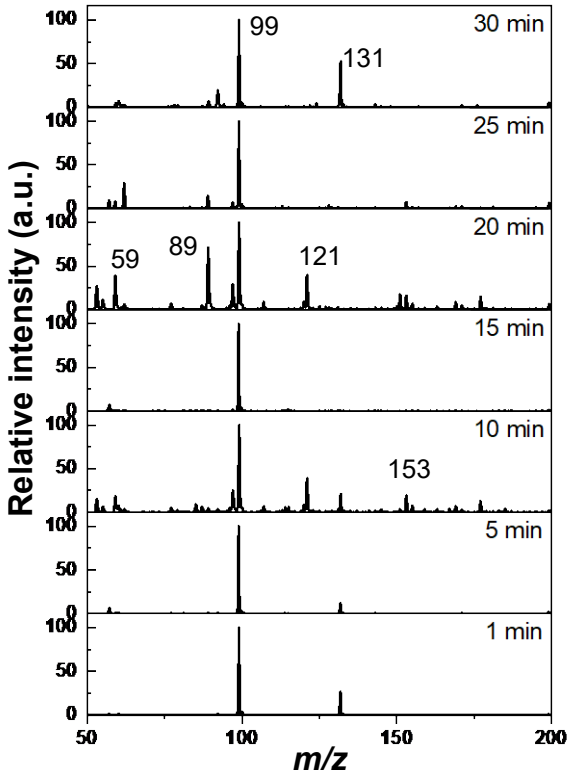

Figure S5. Time-dependent ESI MS measurements of the bulk reaction mixtures. The absence of a peak at *m/z* 143 shows no product formation in bulk.

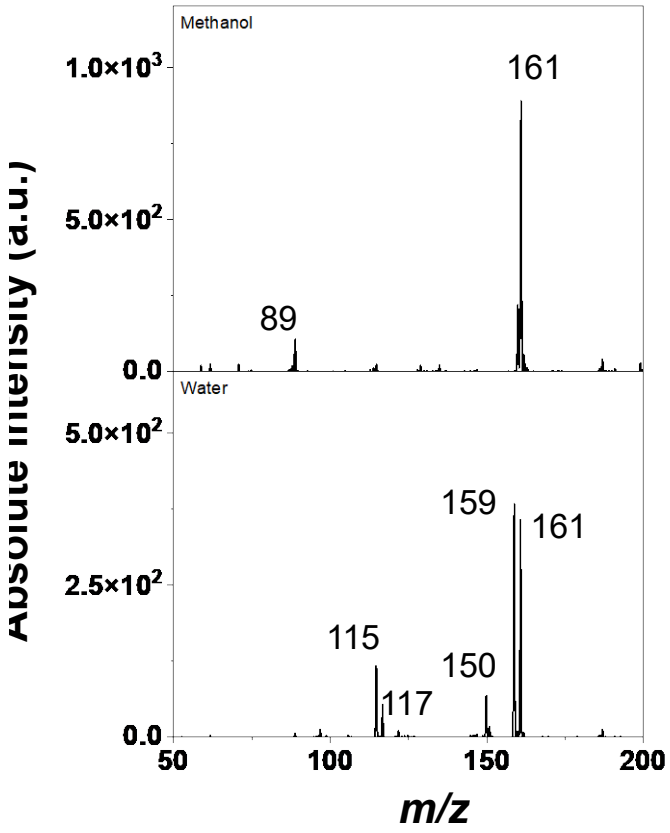

Figure S6. Background mass spectra were recorded using methanol (top) and water (bottom) showing no traces of reagent and product peak at *m/z* 99 and 143, respectively. Peaks that appeared in the mass spectra are either from solvents or from the instrument.

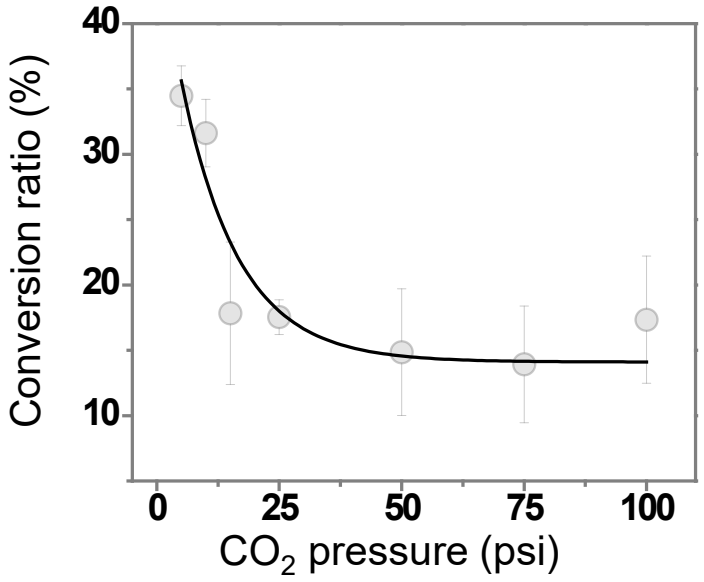

Figure S7. Conversion ratio vs CO_2 gas pressure plot showing that reaction takes place at low CO_2 flow rate which gives enough flight time for the nucleophilic addition reaction.

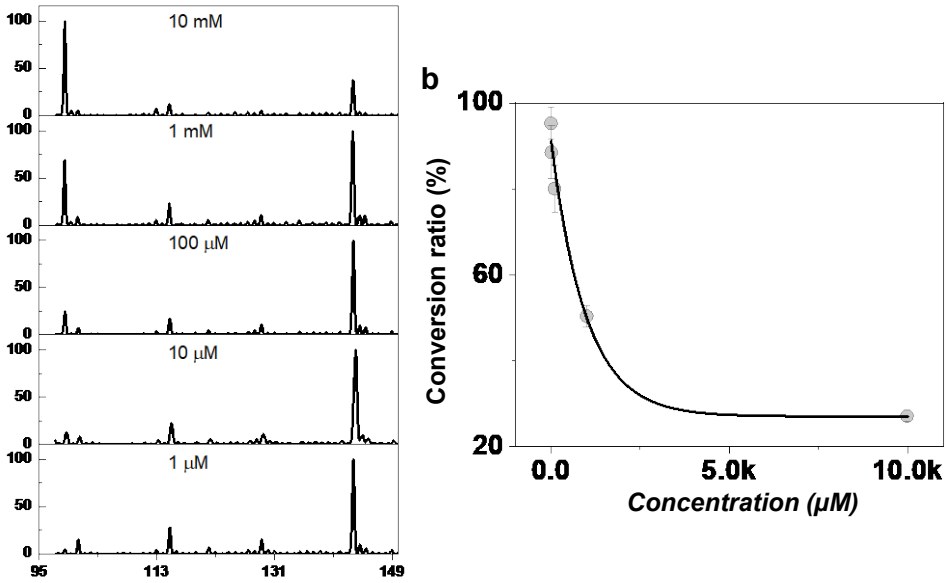

FigureS8. Effect of total reagent concentration in the microdroplet carboxylation reaction. a) Mass spectra collected at different concentration of AcAc varying from 1 μM to 10 mM, respectively. b) shows the C.R.(%) vs concentration plot where we observed that with increasing concentration, relative intensity of the product peak with respect to the reagent peak, decreases until it reaches a plateau.

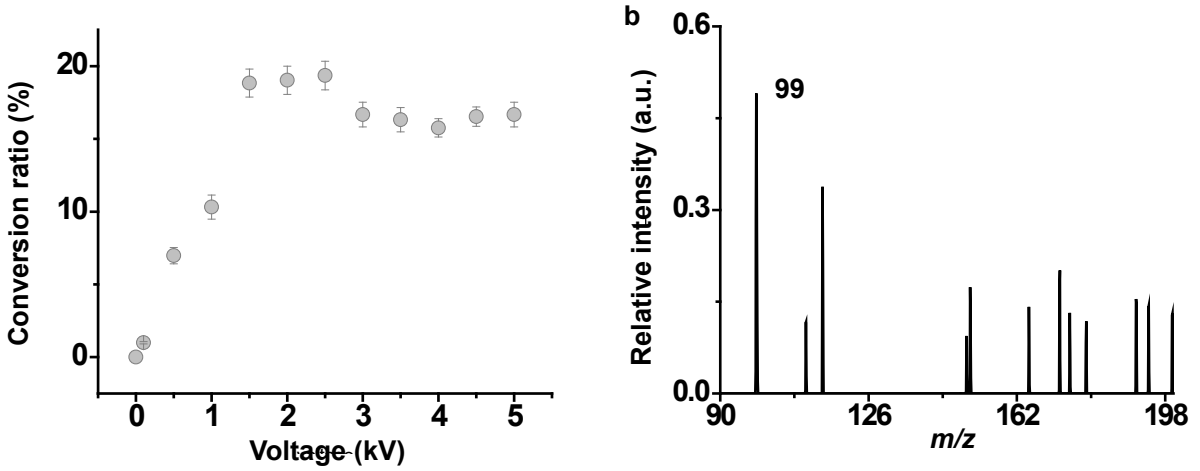

Figure S9. Spray voltage variation experiments a) Effect of spray voltage on the reagent to product conversion ratio of the microdroplet carboxylation reaction. b) Mass spectrum collected at zero applied potential. We observed negligible signal with absolute intensity of 0.6 a.u. A peak at *m/z* 99 maybe due to in-source gas phase ionization. Absence of product peak at *m/z* 143 suggests that the reaction does not occur without the application of potential.

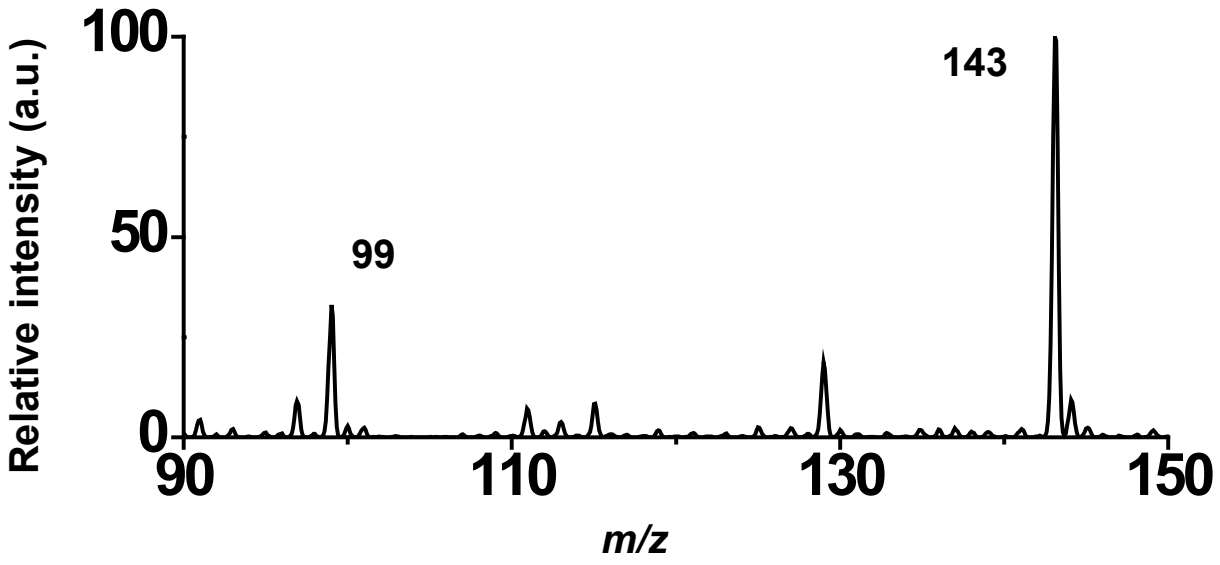

Figure S10. Microdroplet reaction mass spectrometry of reaction mixture containing 1:30 ratio of AcAc and $(NH_4)_2CO_3$.

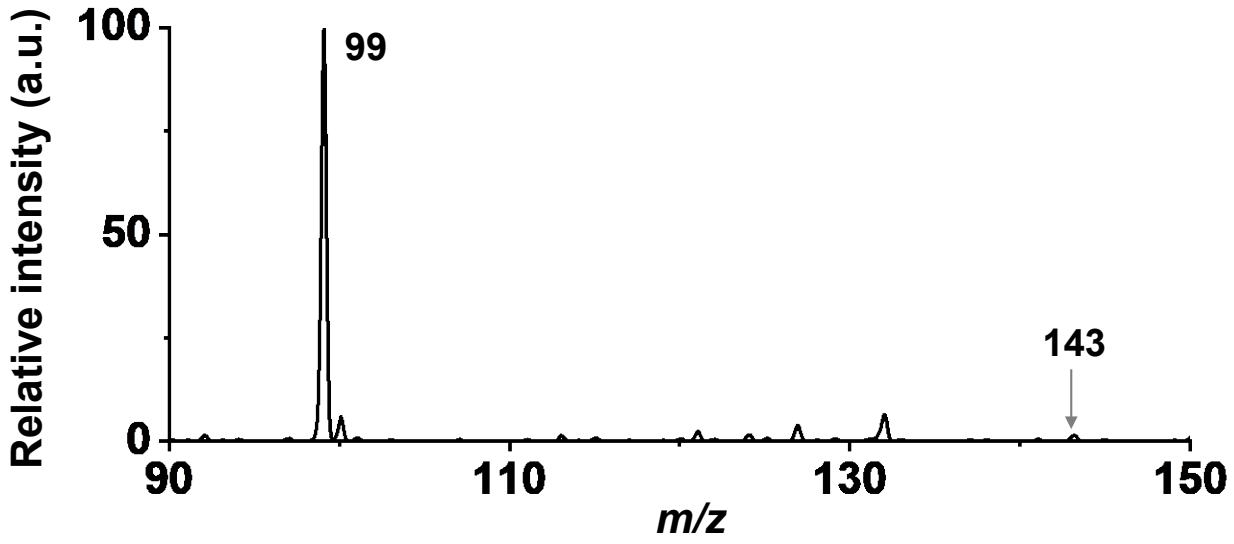

Figure S11. Microdroplet reaction mass spectrometry between AcAc and CO_2 using ambient air nebulization. The experiment was performed using a compressed air cylinder. The CR was 1.4 %.

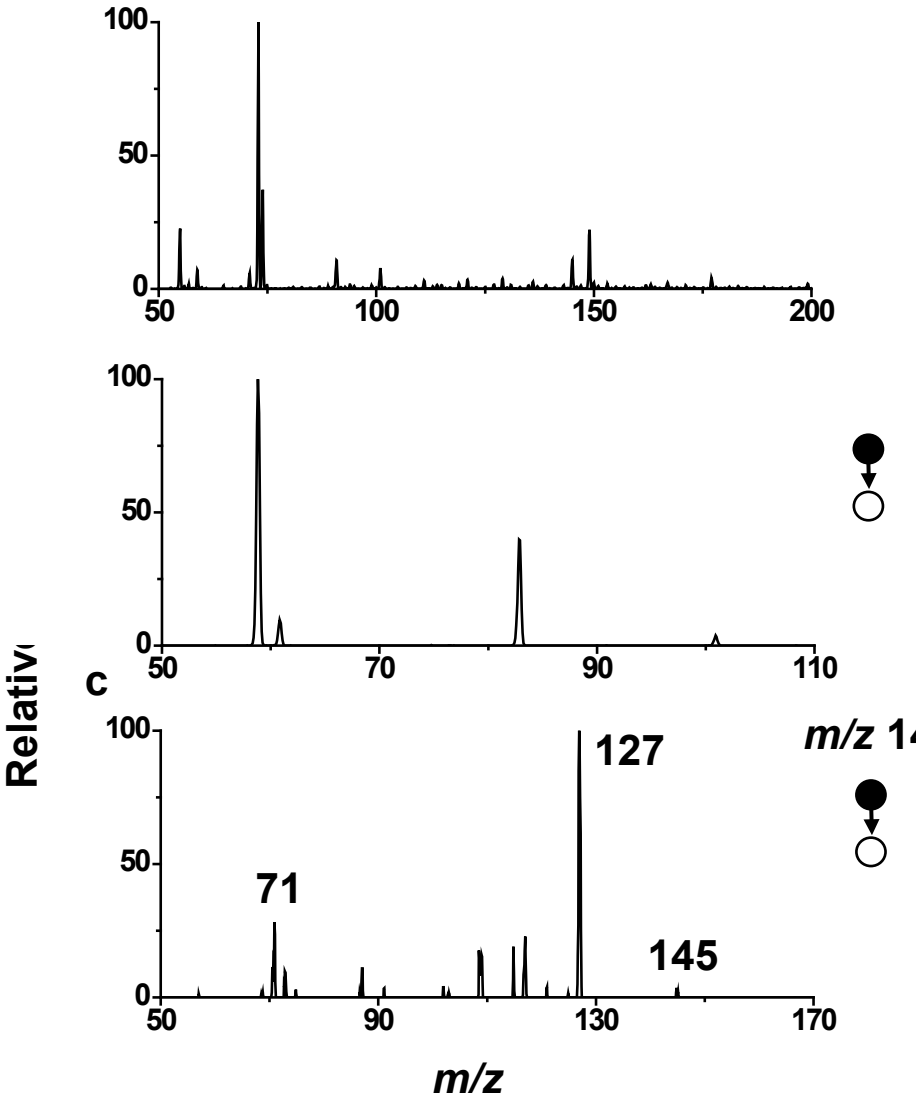

Figure S12. Positive ion mode microdroplet reaction mass spectrometry. a) Mass spectrum of reaction mixture between aqueous AcAc and CO_2 as nebulization gas. b) MS/MS of the reagent peak at *m/z* 101, showing characteristic loss of CH_2CO and H_2O, respectively. C) MS/MS of the peak at *m/z* 145, showing a major loss of a water molecule and a loss resulting in a peak at *m/z* 71. This confirms that the peak at *m/z* 145 does not correspond to the product.

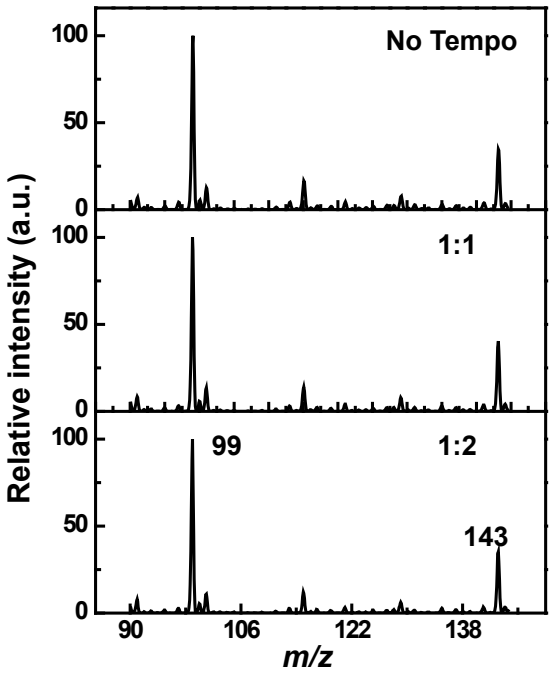

Figure S13. Effect of a radical scavenger i.e., TEMPO on the droplet carboxylation reaction. Mass spectra showing no effect of TEMPO addition with 1:1 and 1:2 ratios of AcAc, confirms that the reaction does not proceed via a radical pathway.

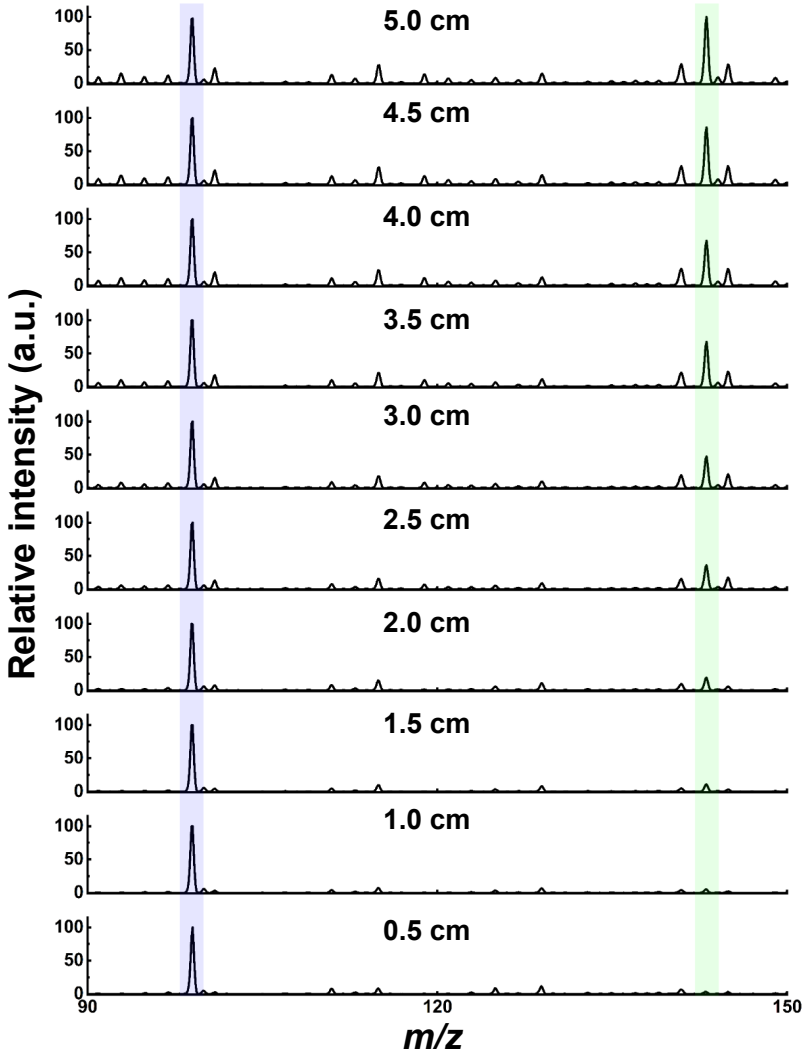

Figure S14. Microdroplet reaction mass spectrometry of reaction between aqueous AcAc and $(NH_4)_2CO_3$. Here tip-to-inlet distance is varied from 0.5 cm up to 5 cm. Negative ion mass spectrums are recorded in gradually increasing distance showing the decrease of the substrate (*m/z* 99) and increase of the product (*m/z* 143).

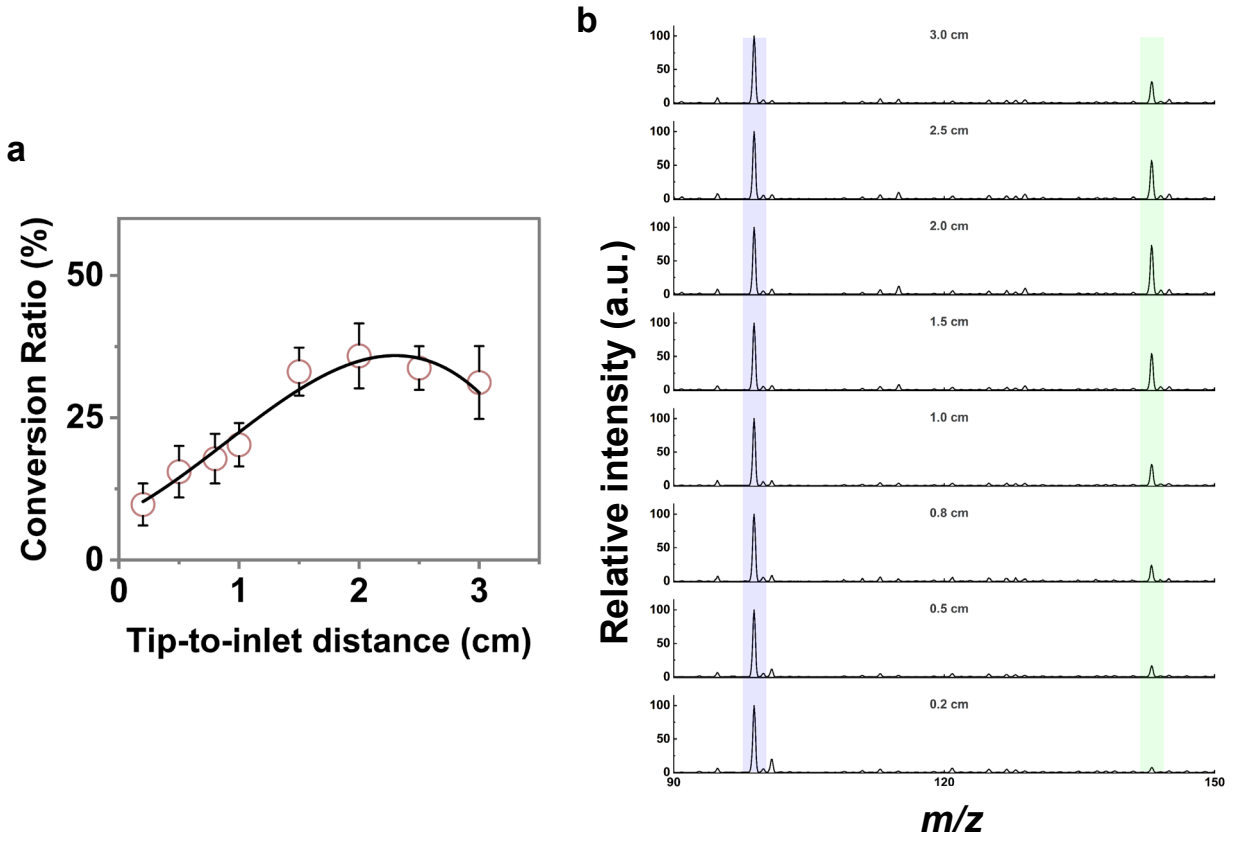

Figure S15. Microdroplet reaction mass spectrometry of reaction between aqueous AcAc and CO_2(g). Here tip-to-inlet distance varies from 0.2 cm up to 3 cm. a) Change of the conversion ratio of the product (*m/z*=143) vs distance. b) Negative ion mass spectrums are recorded at gradually increasing distances showing the increase of the product (*m/z* 143).

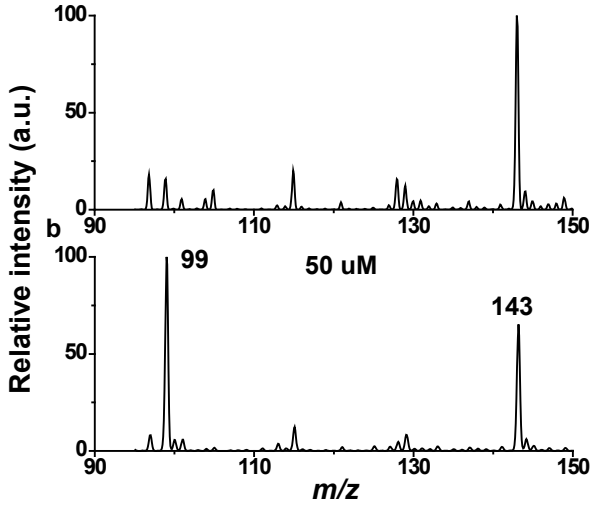

Figure S16. Electrospray emitter tip diameter variation experiments. Online mass spectra collected using two different tip dimeter such as a) 15 µm and b) 50 µm, respectively.

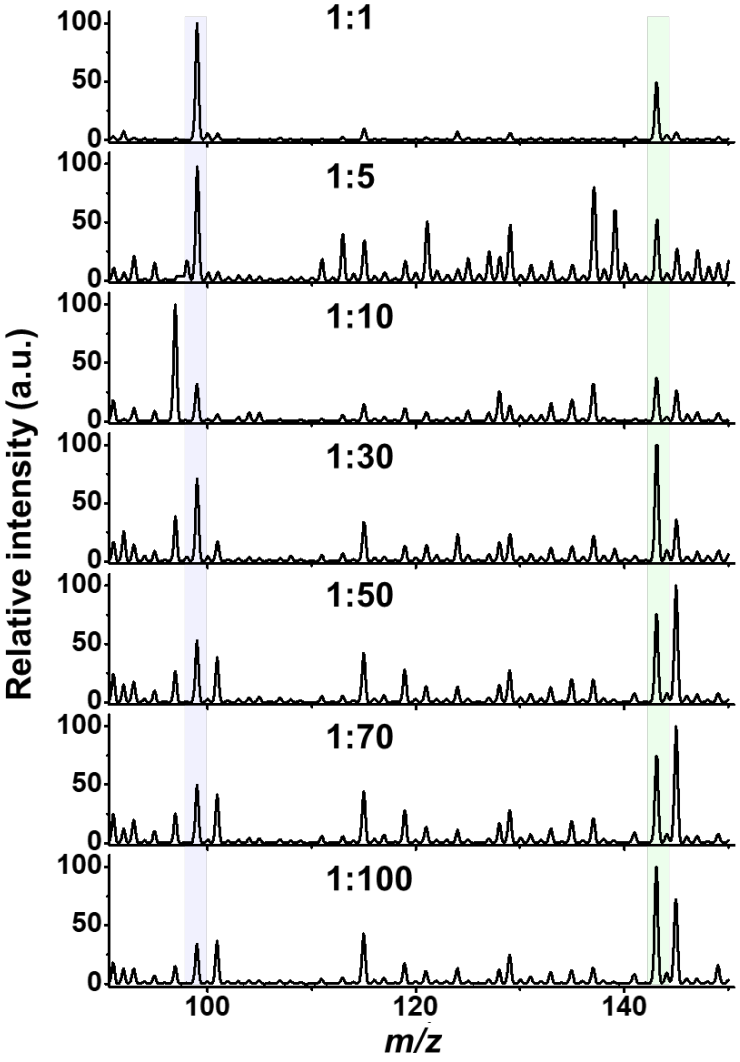

Figure S17. Mass spectra of reaction mixture containing AcAc and $(NH_4)_2CO_3$ at varying bulk ratios of both the reagents.

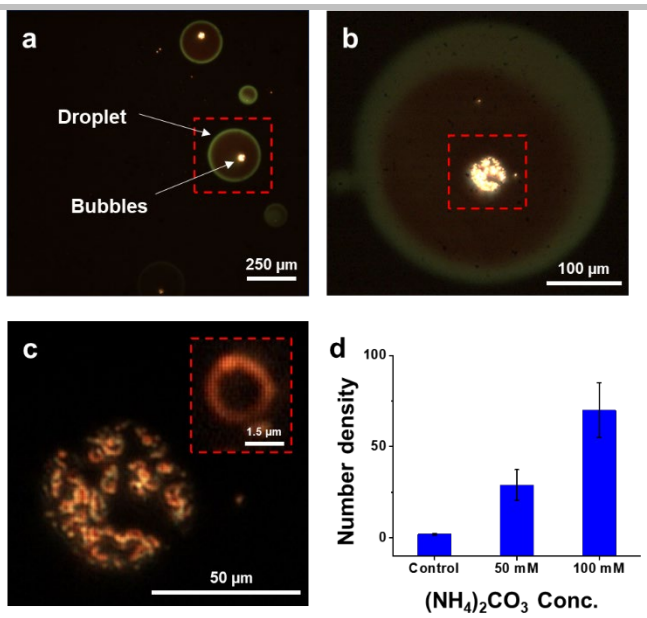

Figure S18. Dark field microscopic images of microdroplets (a) Images of droplet taken on a clean glass slide. (b) Zoomed image of deposited microdroplets shows the aggregated microbubbles inside the microdroplet (indicated in red box), (c) Zoomed image of aggregation of microbubbles inside of the microdroplets, (d) Graph of number density of microbubbles vs $(NH_4)_2CO_3$ clearly indicates the increase in number of microbubbles with increase of $(NH_4)_2CO_3$ concentration.

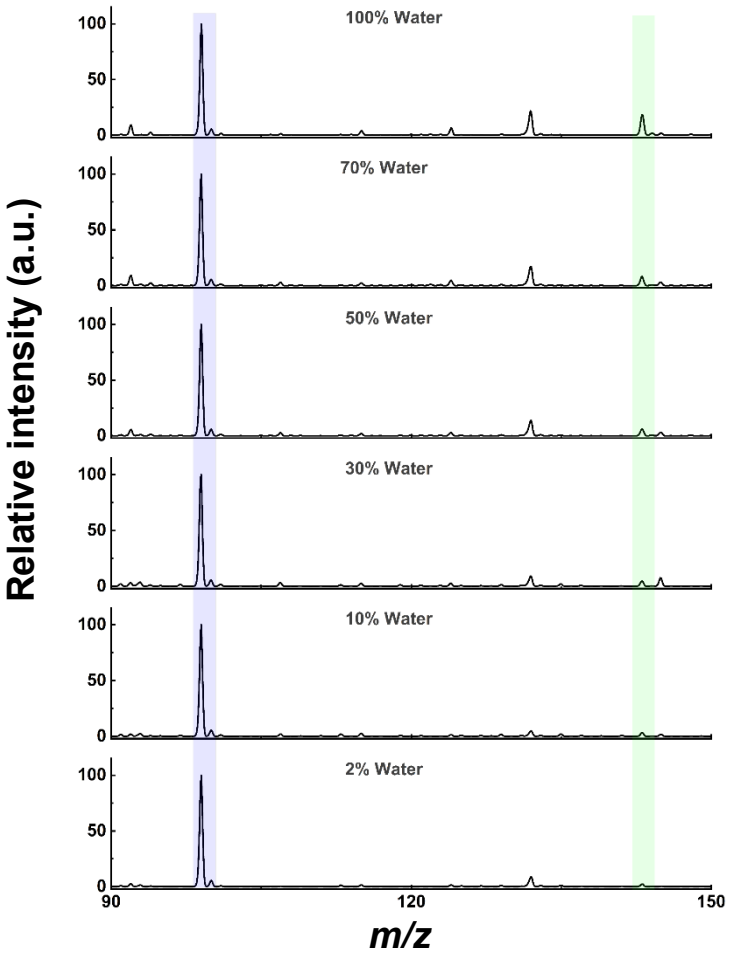

Figure S19. Mass spectrums of the reaction between AcAc and $(NH_4)_2CO_3$ for different solvent compositions (water-methanol mixture). The increase of the percentage of water in the methanol (from 2% to 100%) shows a gradual increment of relative abundance of product in the spectrum.

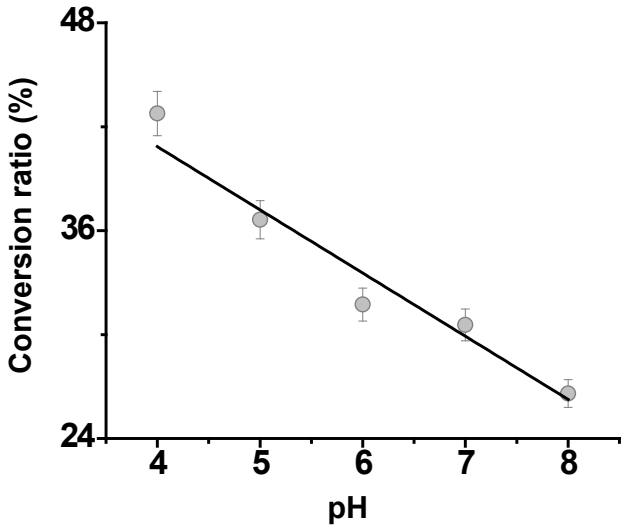

Figure S20. Effect of pH on the reagent to product conversion ratio. Acidic and basic pH solutions were achieved by adding HCl and NaOH, respectively.

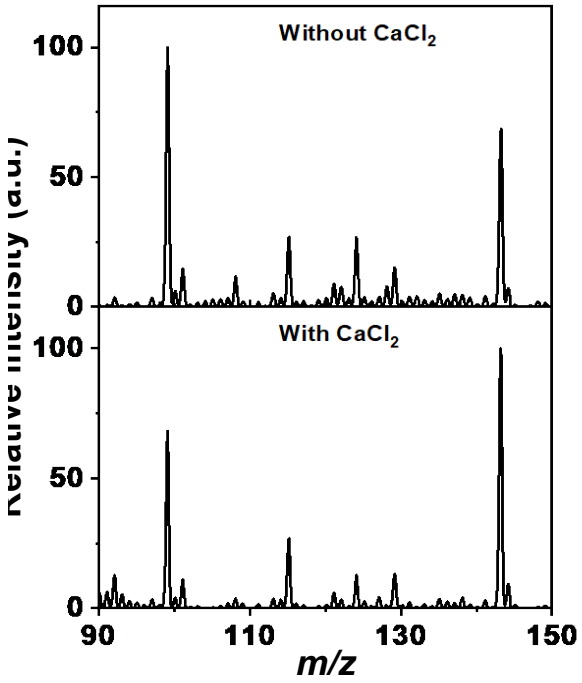

Figure S21. Effect of ionic strength on our microdroplet carboxylation reaction. Ionic strength of the solution was increased by adding a non-interactive salt $CaCl_2$ in the reaction mixture in equimolar ratio with the reagents having 3 mM final concentration of each reagent.

SUPPORTING INFORMATION

Supporting information 3

First-principles density functional theory calculations were conducted to understand the reaction mechanism of converting ketones to ketone carboxylates. Specifically, the reaction barrier for the formation of a C-C bond between the ketone and carbon dioxide molecules was examined. To this end, we optimized the geometries of the reactants, products, intermediates, and transition states at the wB97XD/6-31+g(d,p)[1] level of theory as implemented in the Gaussian16 suite of programs.[2] Furthermore, vibrational analysis was carried out for all the optimized geometries to confirm the nature of the minimum, i.e., the presence of a single imaginary frequency for transition states, and the absence of imaginary frequencies for intermediates. We included the solvent effects by considering the well-established SMD solvation model, which is a continuum solvation model based on the solute's electron density.[3] Finally, to include the effects of hydrogen bonding, we have considered up to three explicit water molecules in our simulations. Free energies of all the complexes were computed at 300 K. Optimized cartesian coordinates of all the complexes are given below.

Cartesian coordinates for all the intermediates and transition states optimized using wB97xD/6-31+g(d,p)

Complex 1 (with 1 H_2O)

C	-2.30671500	-1.13201100	-0.38817600
H	-2.26103700	-1.74819700	-1.29060900
H	-2.73499500	-0.16476500	-0.67778900
H	-2.93987900	-1.60019500	0.36633800
C	-0.93227700	-0.88541300	0.15066500
C	0.12277000	-0.49935000	-0.86990500
H	0.35613000	-1.40166300	-1.44671300
C	1.35893800	0.07116300	-0.21208300
C	2.51771300	-0.84166100	0.00780800
H	3.31642500	-0.34327300	0.55769100
H	2.17465900	-1.73060900	0.54863500
H	2.88562500	-1.18611500	-0.96532600
O	-0.66609500	-0.97690200	1.34220700
O	1.37714600	1.24942800	0.13350200
O	-1.09158900	2.66504400	0.06100400
H	-1.76470400	1.98020000	-0.02188200
H	-0.24436300	2.18170100	0.06395100
H	-0.30613000	0.23598300	-1.55785400

Complex $TS_{1/2}$ (with 1 H_2O)

C	-2.54165500	-0.91122200	-0.45655700
H	-2.96840200	-1.67872300	0.19836400
H	-2.33936900	-1.35697500	-1.43247800
H	-3.28775800	-0.11851500	-0.56566400
C	-1.30150300	-0.34447800	0.20267300
C	-0.04286500	-0.64511300	-0.40972700
H	-0.06953800	-1.36299900	-1.22301100
C	1.23964400	-0.38317600	0.16074600
C	2.40844800	-1.20980800	-0.32082700
H	3.30646200	-0.59053900	-0.38880000
H	2.59724800	-1.99748000	0.41809200
H	2.21192300	-1.68902400	-1.28219800
O	-1.45574000	0.34573400	1.24172600
O	1.46147400	0.51803200	1.01733300
O	0.23137500	2.12238800	-0.87844900
H	-0.61190300	2.60517500	-0.81631600
H	0.66610400	2.13329100	0.00536400
H	0.02595200	1.12933300	-1.01608200

Complex 2 (with 1 H_2O)

C	-2.19744200	-1.56155600	-0.30656400
H	-1.88718200	-2.55377600	-0.63928600
H	-2.65699900	-1.04419000	-1.15721500
H	-2.94588700	-1.64267300	0.48452200
C	-1.03594100	-0.73983600	0.16460400
C	0.27689800	-1.02774900	-0.32970100
H	0.41761600	-1.84817800	-1.02189400
C	1.36691200	-0.28663900	0.05128200
C	2.75178600	-0.52729300	-0.43422400
H	3.40700100	-0.73710300	0.41711800
H	2.78508000	-1.36386400	-1.13235300
H	3.12758700	0.37458300	-0.92776800
O	-1.24315900	0.21827400	0.96086700
O	1.26166900	0.72519700	0.90819100
O	-1.03860900	2.61259000	-0.75407800
H	-1.28008800	1.89145200	-0.15337200
H	0.29951300	0.78741100	1.15983100

H	-0.07914000	2.54629600	-0.82180300

Complex 1 (with 2 H_2O)

C	-2.30671500	-1.13201100	-0.38817600
H	-2.26103700	-1.74819700	-1.29060900
H	-2.73499500	-0.16476500	-0.67778900
H	-2.93987900	-1.60019500	0.36633800
C	-0.93227700	-0.88541300	0.15066500
C	0.12277000	-0.49935000	-0.86990500
H	0.35613000	-1.40166300	-1.44671300
C	1.35893800	0.07116300	-0.21208300
C	2.51771300	-0.84166100	0.00780800
H	3.31642500	-0.34327300	0.55769100
H	2.17465900	-1.73060900	0.54863500
H	2.88562500	-1.18611500	-0.96532600
O	-0.66609500	-0.97690200	1.34220700
O	1.37714600	1.24942800	0.13350200
O	-1.09158900	2.66504400	0.06100400
H	-1.76470400	1.98020000	-0.02188200
H	-0.24436300	2.18170100	0.06395100
H	-0.30613000	0.23598300	-1.55785400

Complex $TS_{1/2}$ (with 2 H_2O)

C	-2.54165500	-0.91122200	-0.45655700
H	-2.96840200	-1.67872300	0.19836400
H	-2.33936900	-1.35697500	-1.43247800
H	-3.28775800	-0.11851500	-0.56566400
C	-1.30150300	-0.34447800	0.20267300
C	-0.04286500	-0.64511300	-0.40972700
H	-0.06953800	-1.36299900	-1.22301100
C	1.23964400	-0.38317600	0.16074600
C	2.40844800	-1.20980800	-0.32082700
H	3.30646200	-0.59053900	-0.38880000
H	2.59724800	-1.99748000	0.41809200
H	2.21192300	-1.68902400	-1.28219800
O	-1.45574000	0.34573400	1.24172600
O	1.46147400	0.51803200	1.01733300
O	0.23137500	2.12238800	-0.87844900
H	-0.61190300	2.60517500	-0.81631600
H	0.66610400	2.13329100	0.00536400
H	0.02595200	1.12933300	-1.01608200

Complex 2 (with 2 H_2O)

C	-2.19744200	-1.56155600	-0.30656400
H	-1.88718200	-2.55377600	-0.63928600
H	-2.65699900	-1.04419000	-1.15721500
H	-2.94588700	-1.64267300	0.48452200
C	-1.03594100	-0.73983600	0.16460400
C	0.27689800	-1.02774900	-0.32970100
H	0.41761600	-1.84817800	-1.02189400
C	1.36691200	-0.28663900	0.05128200
C	2.75178600	-0.52729300	-0.43422400
H	3.40700100	-0.73710300	0.41711800
H	2.78508000	-1.36386400	-1.13235300
H	3.12758700	0.37458300	-0.92776800
O	-1.24315900	0.21827400	0.96086700
O	1.26166900	0.72519700	0.90819100
O	-1.03860900	2.61259000	-0.75407800
H	-1.28008800	1.89145200	-0.15337200
H	0.29951300	0.78741100	1.15983100
H	-0.07914000	2.54629600	-0.82180300

Complex 1 (with 3 H_2O)

C	-2.30671500	-1.13201100	-0.38817600
H	-2.26103700	-1.74819700	-1.29060900
H	-2.73499500	-0.16476500	-0.67778900
H	-2.93987900	-1.60019500	0.36633800
C	-0.93227700	-0.88541300	0.15066500
C	0.12277000	-0.49935000	-0.86990500
H	0.35613000	-1.40166300	-1.44671300
C	1.35893800	0.07116300	-0.21208300
C	2.51771300	-0.84166100	0.00780800
H	3.31642500	-0.34327300	0.55769100
H	2.17465900	-1.73060900	0.54863500
H	2.88562500	-1.18611500	-0.96532600
O	-0.66609500	-0.97690200	1.34220700
O	1.37714600	1.24942800	0.13350200
O	-1.09158900	2.66504400	0.06100400
H	-1.76470400	1.98020000	-0.02188200
H	-0.24436300	2.18170100	0.06395100
H	-0.30613000	0.23598300	-1.55785400

Complex $TS_{1/2}$ (with 3 H_2O)

C	-2.54165500	-0.91122200	-0.45655700
H	-2.96840200	-1.67872300	0.19836400
H	-2.33936900	-1.35697500	-1.43247800
H	-3.28775800	-0.11851500	-0.56566400
C	-1.30150300	-0.34447800	0.20267300
C	-0.04286500	-0.64511300	-0.40972700
H	-0.06953800	-1.36299900	-1.22301100
C	1.23964400	-0.38317600	0.16074600
C	2.40844800	-1.20980800	-0.32082700
H	3.30646200	-0.59053900	-0.38880000
H	2.59724800	-1.99748000	0.41809200
H	2.21192300	-1.68902400	-1.28219800
O	-1.45574000	0.34573400	1.24172600
O	1.46147400	0.51803200	1.01733300
O	0.23137500	2.12238800	-0.87844900
H	-0.61190300	2.60517500	-0.81631600
H	0.66610400	2.13329100	0.00536400
H	0.02595200	1.12933300	-1.01608200

Complex 2 (with 3 H_2O)

C	-2.19744200	-1.56155600	-0.30656400
H	-1.88718200	-2.55377600	-0.63928600
H	-2.65699900	-1.04419000	-1.15721500
H	-2.94588700	-1.64267300	0.48452200
C	-1.03594100	-0.73983600	0.16460400
C	0.27689800	-1.02774900	-0.32970100
H	0.41761600	-1.84817800	-1.02189400
C	1.36691200	-0.28663900	0.05128200
C	2.75178600	-0.52729300	-0.43422400
H	3.40700100	-0.73710300	0.41711800
H	2.78508000	-1.36386400	-1.13235300
H	3.12758700	0.37458300	-0.92776800
O	-1.24315900	0.21827400	0.96086700
O	1.26166900	0.72519700	0.90819100
O	-1.03860900	2.61259000	-0.75407800
H	-1.28008800	1.89145200	-0.15337200
H	0.29951300	0.78741100	1.15983100
H	-0.07914000	2.54629600	-0.82180300

SUPPORTING INFORMATION

Complex 3 (with 3 H_2O)

C	2.25346900	0.72328500	1.85411900
H	1.71734500	0.96571100	2.77355600
H	2.68072800	1.62430500	1.40976400
H	3.07569700	0.04398800	2.10932200
C	1.37032300	0.02863700	0.86660700
C	0.27425100	-0.76484200	1.33332000
H	0.09631100	-0.85261100	2.39744000
C	-0.58063500	-1.39358500	0.46546600
C	-1.75588600	-2.20126200	0.88226400
H	-1.85432200	-2.22267300	1.96748000
H	-2.66381200	-1.77793900	0.43997600
H	-1.64904600	-3.22295300	0.50409000
O	1.61885400	0.13345500	-0.36842600
O	-0.43024000	-1.30185200	-0.85511200
C	-1.80708800	1.68975700	0.45598500
O	-2.65922400	1.22706900	1.10212800
O	-0.95949100	2.16499300	-0.18604200
O	-2.85046400	-0.13456400	-2.00505700
H	-3.45014200	-0.16803600	-1.25116600
H	-2.03104700	-0.53784200	-1.67808300
H	0.36890000	-0.72882400	-1.01839700
O	2.26357500	2.68228100	-1.36708500
H	1.42255200	3.13866100	-1.25444500
H	2.10620500	1.78957700	-1.00693900
O	2.68259900	-2.52500400	-1.13524000
H	1.80973200	-2.92778900	-1.06029800
H	2.51942100	-1.58653400	-0.96020600

Complex 4 (with 3 H_2O)

C	0	2.49034200	2.07666800	-0.53848700
H	0	2.22111900	3.05177200	-0.94681600
H	0	2.90953900	1.46167600	-1.34291700
H	0	3.26920800	2.19756300	0.22005000
C	0	1.31625700	1.34226700	0.06138100
C	0	0.03012600	1.88179600	-0.15621400
H	0	0.02532400	2.81816000	-0.70269400
C	0	-1.25097300	1.33337100	0.06722600
C	0	-2.43141700	2.04666200	-0.54546300
H	0	-2.81944500	1.42988400	-1.36469100
H	0	-3.22744900	2.14203700	0.19846600
H	0	-2.17680300	3.03088700	-0.94106900
O	0	1.60512600	0.26174500	0.67753700
O	0	-1.52982700	0.25829400	0.69725600
C	0	-0.03572100	-1.82330100	-0.72853100
O	0	-0.02282700	-1.18119500	-1.70075300
O	0	-0.04583900	-2.50478800	0.21647500
O	-1	0.04759600	-0.35784400	2.48007700
H	-1	-0.75622200	-0.19507300	1.93467000
H	-1	0.03798200	-1.29592300	2.77670800
H	-1	0.85077500	-0.20453200	1.93313200
O	0	-3.45940500	-1.38515000	-0.40717900
H	0	-3.81581200	-0.89012600	-1.15284000
H	0	-2.80852600	-0.77854300	0.00286000
O	0	3.38722700	-1.50261400	-0.48915000
H	0	2.79090700	-0.84494200	-0.07554000
H	0	2.93131800	-1.77521200	-1.29289800

Complex $TS_{4/5}$ (with 3 H_2O)

C	0	2.39775200	-1.79099900	-0.58133800
H	0	2.34382000	-2.23545600	0.41652900

H	0	3.36025200	-1.29720800	-0.72081800
H	0	2.30236600	-2.60621500	-1.30717900
C	0	1.27142800	-0.81395900	-0.79255800
C	0	-0.02146500	-1.25348200	-0.33130800
H	0	-0.00207500	-2.28844600	-0.00426000
C	0	-1.34586900	-0.85000900	-0.74441800
C	0	-2.43813200	-1.84667900	-0.45628300
H	0	-3.41700700	-1.37901100	-0.56977800
H	0	-2.35397900	-2.68215300	-1.16014900
H	0	-2.33190000	-2.25762300	0.55182100
O	0	1.55502500	0.29739900	-1.30770700
O	0	-1.67416300	0.23463300	-1.28232300
C	0	0.03695800	-0.34435000	1.59949800
O	0	-0.04177100	0.83470000	1.41550900
O	0	0.13401300	-1.26612500	2.35100000
O	-1	-0.08741600	2.15476100	-1.40267900
H	-1	-0.88794200	1.59377000	-1.34285900
H	-1	-0.08810600	2.78866700	-0.65521500
H	-1	0.70824300	1.58764500	-1.33882800
O	0	-2.93365000	1.71329600	0.88962800
H	0	-2.07296900	1.59142600	1.31222300
H	0	-2.83797400	1.22783700	0.05646400
O	0	3.12839100	1.62055500	0.73902200
H	0	2.74545900	1.20671500	-0.05110600
H	0	2.48435500	1.43317100	1.43198000

Complex 5 (with 3 H_2O)

C	0	2.60458000	0.97642600	1.01280200
H	0	3.31069200	0.58866800	0.26970800
H	0	2.99531900	0.82281400	2.01857000
H	0	2.48259500	2.04539300	0.80492900
C	0	1.29535900	0.28078900	0.83551200
C	0	0.56217900	0.55840700	-0.48021700
H	0	1.32622000	0.78461600	-1.23128000
C	0	-0.32783900	1.79742500	-0.33480500
C	0	-0.05596500	2.93033800	-1.26052800
H	0	-0.75467400	3.75051700	-1.09699800
H	0	0.97621200	3.26726700	-1.11111600
H	0	-0.12267000	2.56619000	-2.29174900
O	0	0.83281300	-0.45864300	1.69590600
O	0	-1.22121300	1.85002200	0.50660600
C	0	-0.23375600	-0.65075200	-1.03679900
O	0	-1.36533100	-0.41581100	-1.53651000
O	0	0.32969000	-1.77142200	-0.99245800
O	-1	-1.82914300	-0.33413300	1.78875800
H	-1	-1.74509400	0.54659800	1.35441800
H	-1	-2.37995100	-0.91145700	1.21170200
H	-1	-0.93670300	-0.73660300	1.88471000
O	0	-3.12616700	-1.75557900	0.09573500
H	0	-2.62893600	-1.39641400	-0.67053600
H	0	-4.03745700	-1.46077700	-0.01945300
O	0	3.01353100	-2.28095000	-0.67270000
H	0	3.31229000	-1.83398600	0.12661900
H	0	2.06137300	-2.05650200	-0.74801400

Complex $TS_{5/6}$ (with 3 H_2O)

C	2.70752400	0.94511200	0.89273800
H	3.38129800	0.57261700	0.11269900
H	3.14064200	0.76695500	1.87705400
H	2.58039100	2.01898900	0.71740700
C	1.39321300	0.24684600	0.75458800

C	0.59461800	0.57371300	-0.50887000
H	1.30397100	0.77731500	-1.31790700
C	-0.24610400	1.83501200	-0.26016100
C	-0.16418300	2.90886800	-1.29030700
H	-0.85099900	3.72445600	-1.06383400
H	0.86726600	3.27839500	-1.32544600
H	-0.38165800	2.48121700	-2.27471300
O	0.96631000	-0.52457600	1.60032800
O	-0.93672100	1.92879500	0.74587200
C	-0.30236000	-0.58229500	-0.97433800
O	-1.49346100	-0.26350200	-1.32651500
O	0.15880800	-1.73395300	-1.00392500
O	-1.89573500	-0.51871100	1.95038800
H	-1.71133500	0.37613200	1.60761700
H	-2.72447600	-1.23292600	0.81076800
H	-1.01095200	-0.92102500	1.93690700
O	-3.05684500	-1.60324900	-0.07733600
H	-2.39994700	-1.06079600	-0.78647100
H	-3.97689500	-1.32761700	-0.20166900
O	2.86178800	-2.38395500	-0.76984000
H	3.13562000	-2.08780300	0.10527200
H	1.91765900	-2.13623200	-0.83135700

Complex 6 (with 3 H_2O)

C	-2.60890200	1.72869900	-1.07581900
H	-1.90278300	2.04612200	-1.84820800
H	-3.02259200	2.59053800	-0.55184800
H	-3.41448600	1.18121900	-1.58009100
C	-1.95608400	0.79109200	-0.11528200
C	-1.08143200	-0.31727100	-0.72105100
H	-1.54112400	-0.66746300	-1.65262400
C	-0.98402700	-1.49684800	0.25062900
C	-2.17428500	-2.39643400	0.31446300
H	-2.11480100	-3.05074900	1.18433000
H	-3.10304900	-1.81970200	0.32676800
H	-2.18194100	-3.00138700	-0.60024900
O	-2.10255100	0.85824900	1.09406400
O	0.02080600	-1.68191000	0.91972800
C	0.29360900	0.23939900	-1.03797300
O	1.03501200	-0.58669400	-1.74230700
O	0.67344700	1.33777000	-0.65365100
O	2.63781000	-0.44280700	1.38735700
H	1.85981400	-0.97652500	1.15605100
H	3.33022800	-0.10010800	-0.23059400
H	2.23555200	0.37718700	1.73295700
O	3.50691500	0.04712900	-1.18865500
H	2.00015500	-0.29444100	-1.69851000
H	4.12454800	-0.64640600	-1.44899000
O	0.96071300	1.72926500	2.14606000
H	0.67370400	1.74217800	1.21743500
H	0.26630000	1.23970100	2.60300200

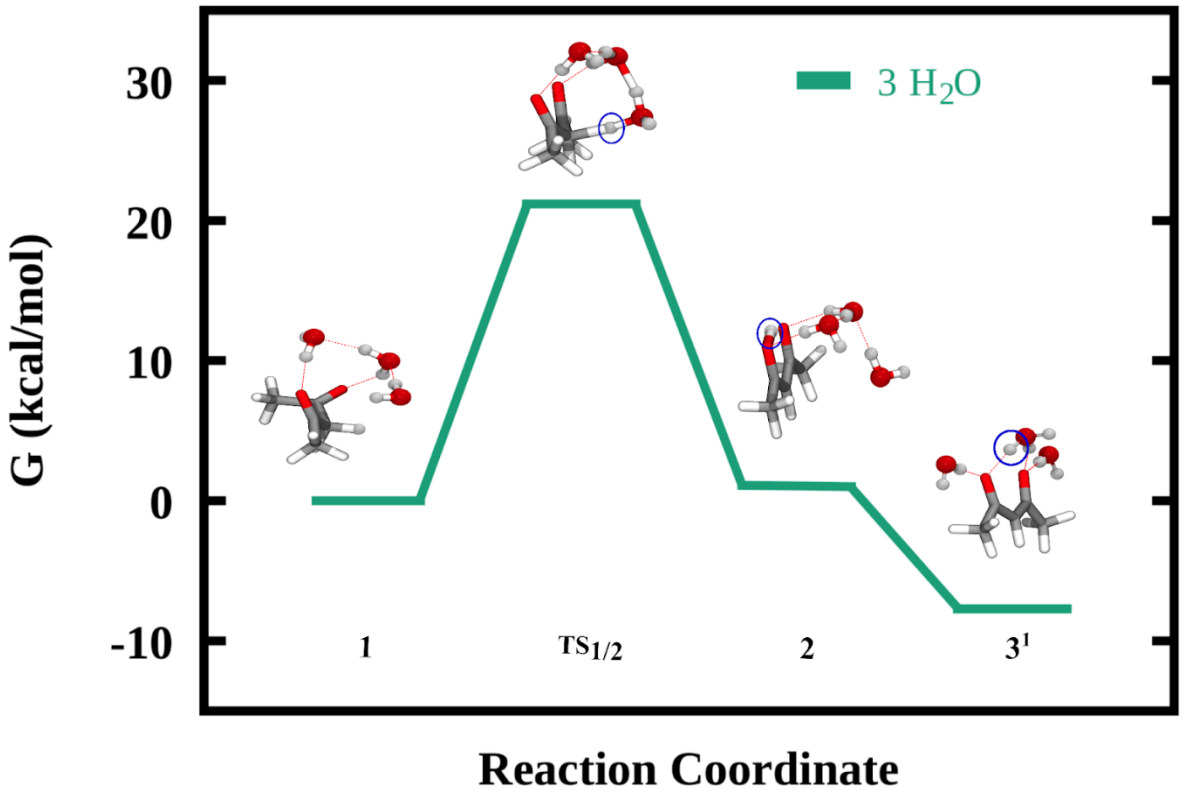

Figure S22. Free energy landscape for keto-enol transformation over AcAc.

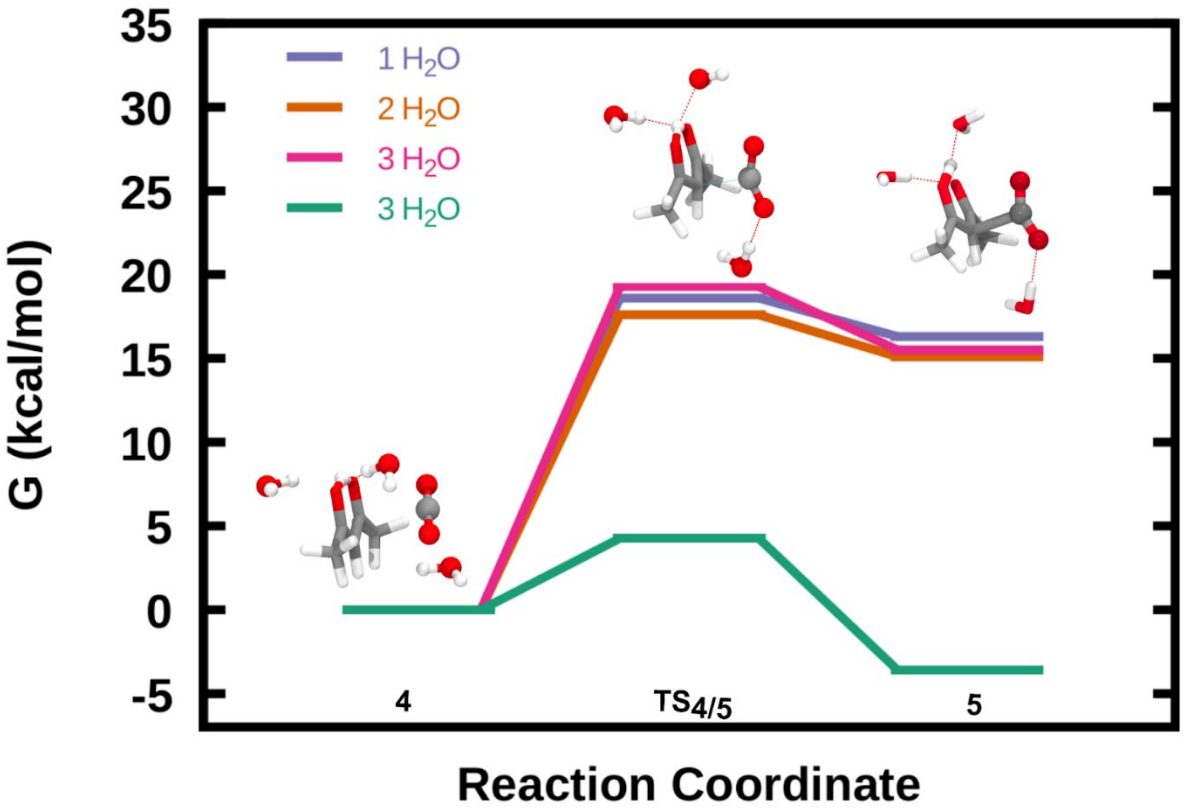

Figure S23: Free energy landscape for C-C bond formation in neutral and negatively charged microdroplets.

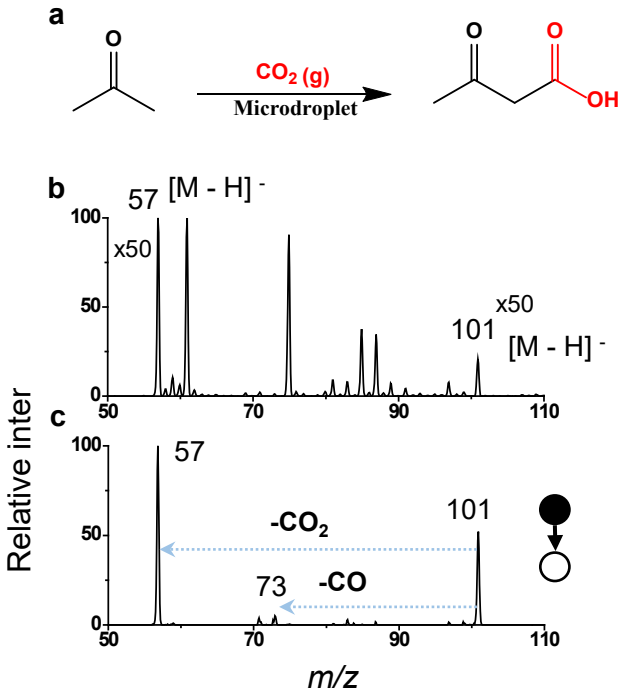

Figure S24. Microdroplet reaction mass spectrometry of reaction mixture containing 1:1 acetone and $(NH_4)_2CO_3$ ratio. a) Reaction scheme between acetone and $(NH_4)_2CO_3$ b) Negative ion mass spectrum of acetone and $(NH_4)_2CO_3$. shows the carboxylated product at *m/z* 101. The calculated CR is 17%. c) MS/MS spectrum of the product shows neutral losses at 57 and 73, which are CO_2 (*m/z* 44) and CO (*m/z* 28) losses, respectively.

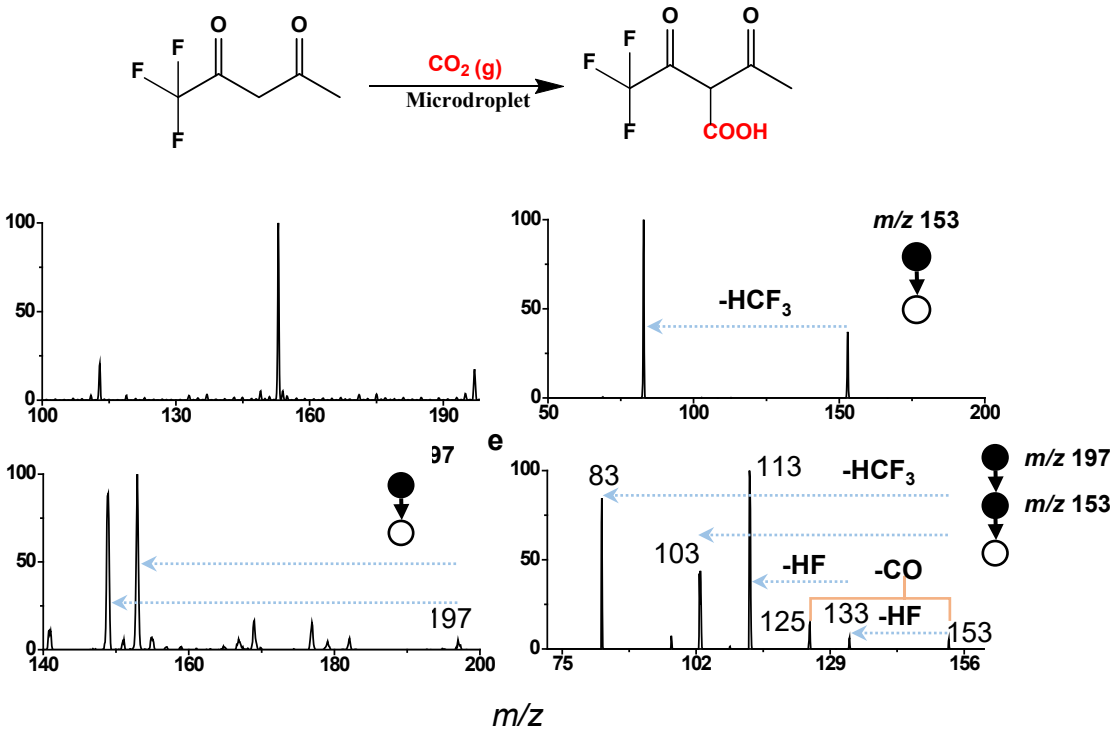

Figure S25. Microdroplet reaction mass spectrometry of reaction mixture containing 1:1 ratio of 1,1,1-trifluoro-5,5-dimethyl-2,4-hexanedione and $(NH_4)_2CO_3$. a) Reaction scheme between 1,1,1-trifluoro-5,5-dimethyl-2,4-hexanedione and $(NH_4)_2CO_3$. b) Negative ion mass spectrum of 1,1,1-trifluoro-5,5-dimethyl-2,4-hexanedione and $(NH_4)_2CO_3$ shows the carboxylated product at *m/z*=191 (the corresponding peak is zoomed to 10 times). The calculated CR is 1.7% c) MS/MS spectrum of the substrate (*m/z* 153) d) MS/MS spectrum of the product (*m/z* 197) e) MS/MS/MS spectrum of the product.

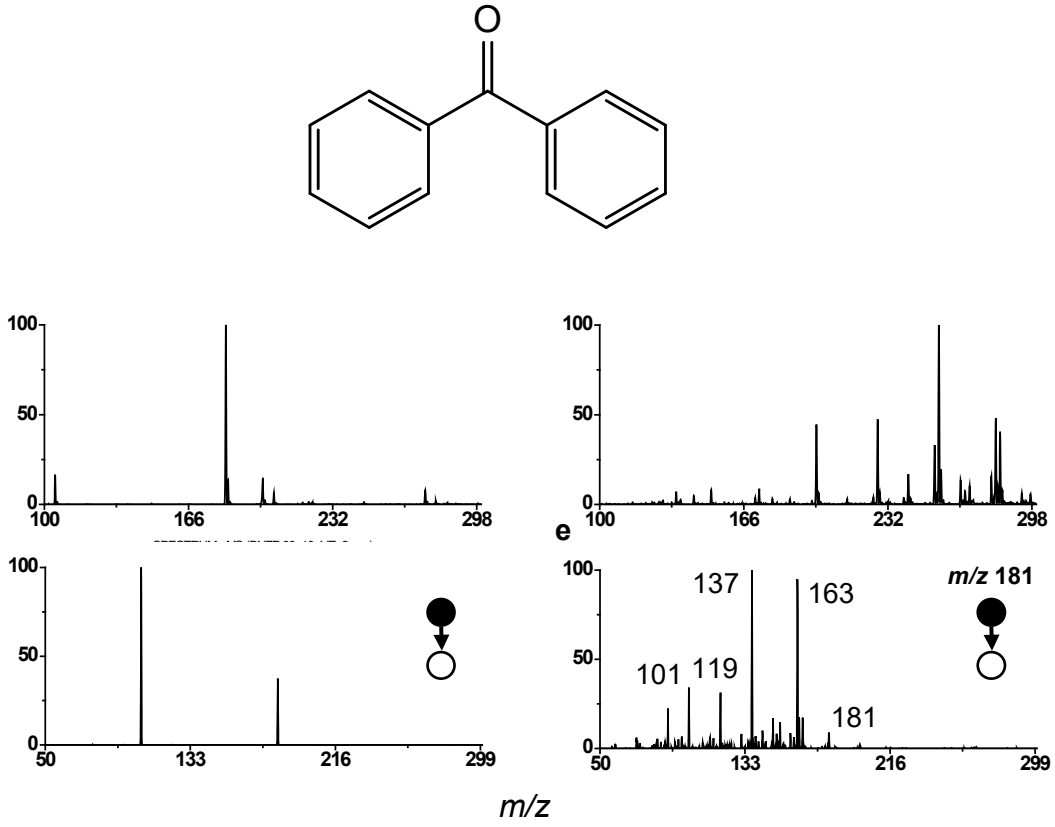

Figure S26. Microdroplet reaction mass spectrometry of reaction mixture containing 1:1 ratio of benzophenone and $(NH_4)_2CO_3$. a) Structure of benzophenone shows unavailability of sp^3 C-H. b) Positive ion mass spectrum of benzophenone and $(NH_4)_2CO_3$. shows the absence of carboxylated product c) MS/MS spectrum of benzophenone (*m/z* 183) in positive mode. d) Negative ion mass spectrum of benzophenone and $(NH_4)_2CO_3$ shows the absence of the peak for benzophenone itself as it is not ionized in negative mode. e) MS/MS spectrum for the *m/z* 181 does not correspond to the molecular ion of benzophenone.

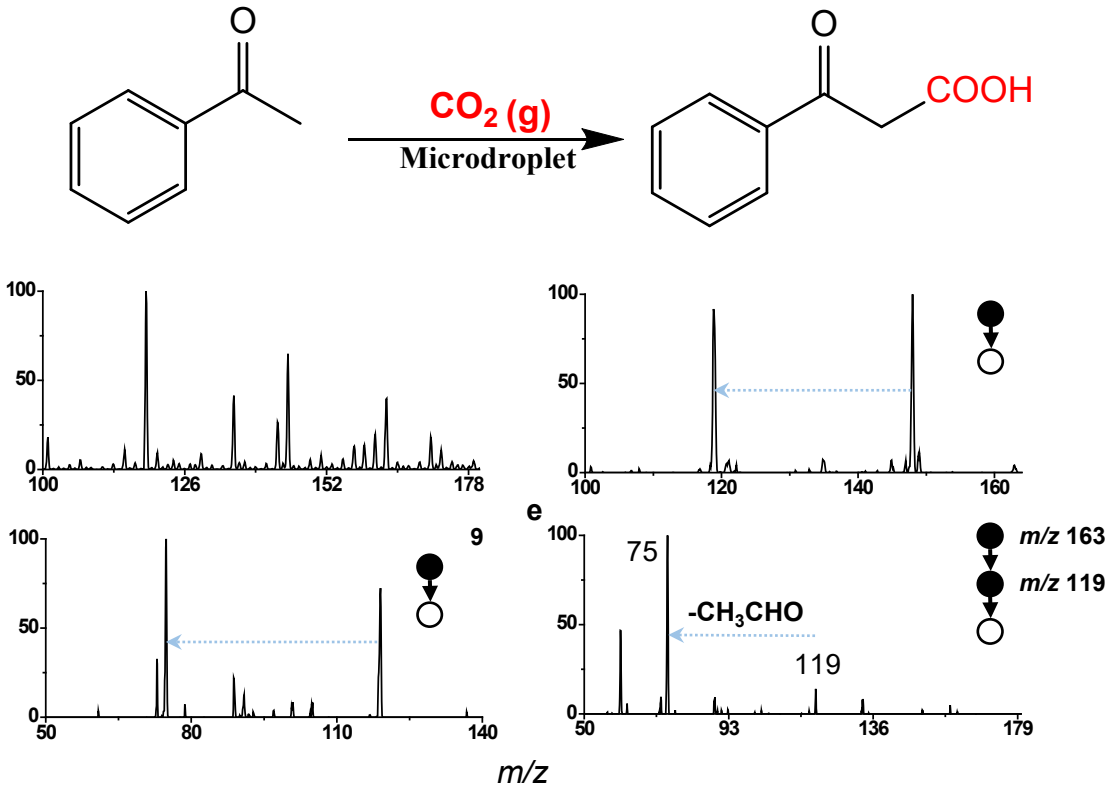

Figure S27. Microdroplet reaction mass spectrometry of reaction mixture containing 1:1 ratio of acetophenone and $(NH_4)_2CO_3$. a) Reaction scheme between acetophenone and $(NH_4)_2CO_3$. b) Negative ion mass spectrum of acetophenone and $(NH_4)_2CO_3$ shows the carboxylated product at *m/z* 163. The calculated CR is 28% c) MS/MS spectrum of the substrate (*m/z* 119). d) MS/MS spectrum of the product (*m/z* 163) e) MS/MS/MS spectrum of the product.

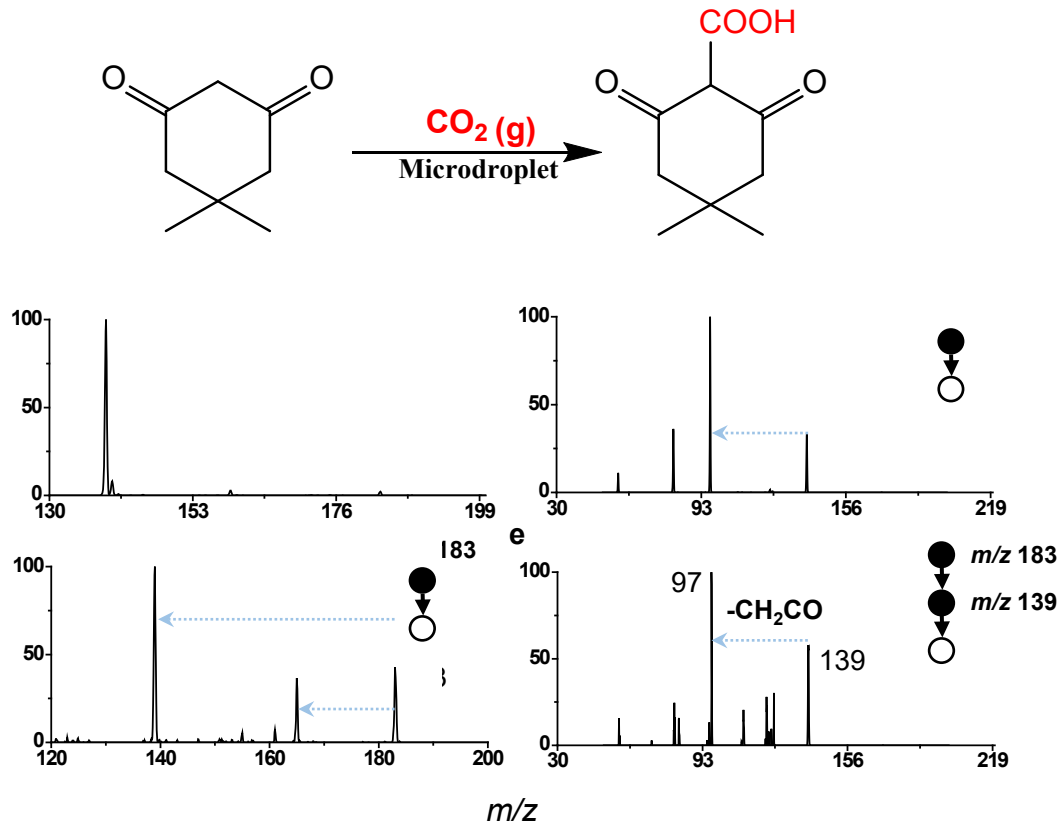

Figure S28. Microdroplet reaction mass spectrometry of reaction mixture containing 1:1 ratio of dimedone (5,5-dimethylcyclohexane-1,3-dione) and $(NH_4)_2CO_3$. a) Reaction scheme between dimedone and $(NH_4)_2CO_3$ b) Negative ion mass spectrum of dimedone and $(NH_4)_2CO_3$ shows the carboxylated product at *m/z* 183 (corresponding peak is zoomed to 100 times). The calculated CR is 0.02%. c) MS/MS spectrum of the substrate (*m/z* 139) d) MS/MS spectrum of the product (*m/z* 183) e) MS/MS/MS spectrum of the product.

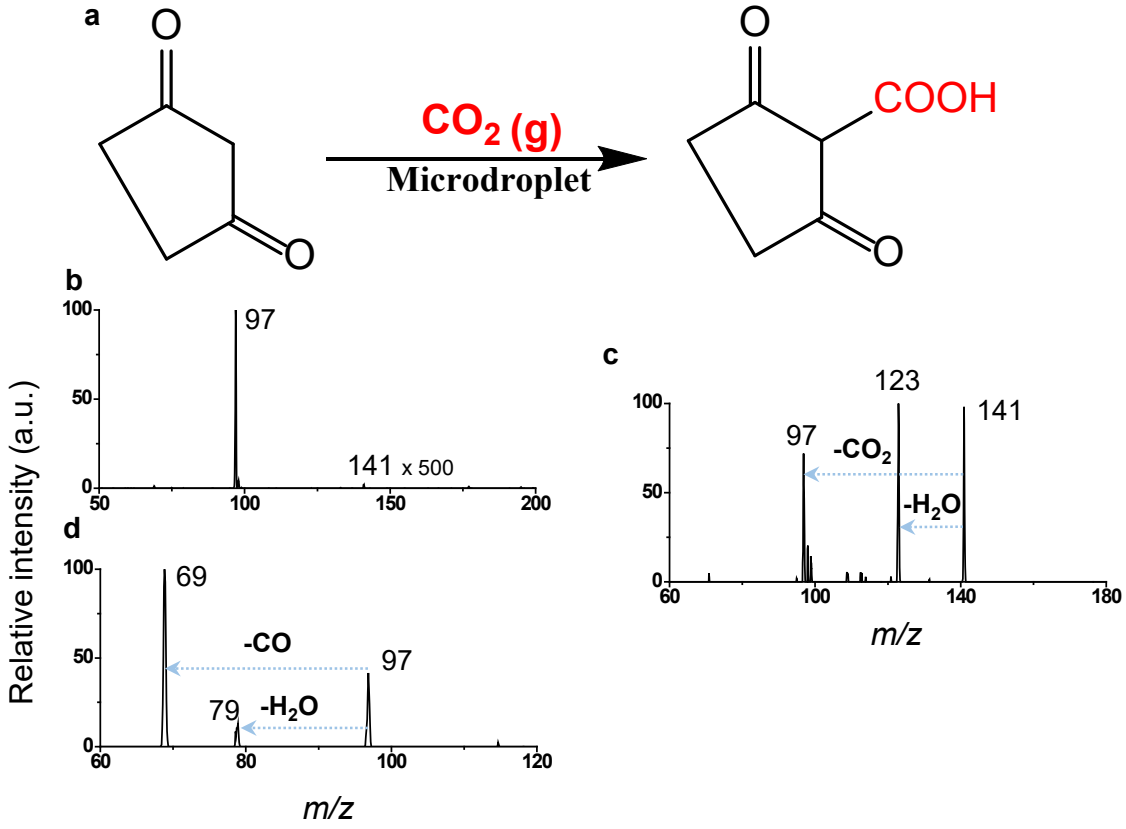

Figure S29. Microdroplet reaction mass spectrometry of reaction mixture containing 1:1 ratio of cyclopentane-1,3-dione and $(NH_4)_2CO_3$. a) Reaction scheme between of cyclopentane-1,3-dione and $(NH_4)_2CO_3$. b) Negative ion mass spectrum of cyclopentane-1,3-dione and $(NH_4)_2CO_3$. shows the carboxylated product at *m/z* 141 (the corresponding peak is zoomed to 500 times). The calculated CR is 0.008%. c) MS/MS spectrum of the substrate (*m/z* 139) d) MS/MS spectrum of the product (*m/z* 141).

Keto-enol tautomerism

a) Acetylacetone

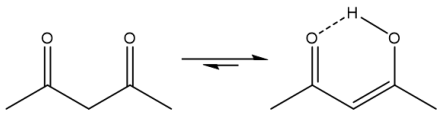

b) cyclopentane-1,3-dione

c) 5,5-dimethylcyclohexane-1,3-dione

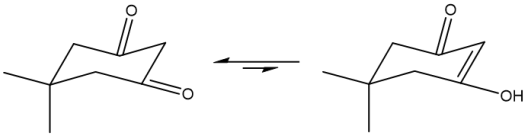

Scheme S2. Scheme showing keto-enol tautomerism among a) AcAc, b) cyclopentane-1,3-dione, and c) 5,5-dimethyl-cyclohexane-1,3-dione, respectively.

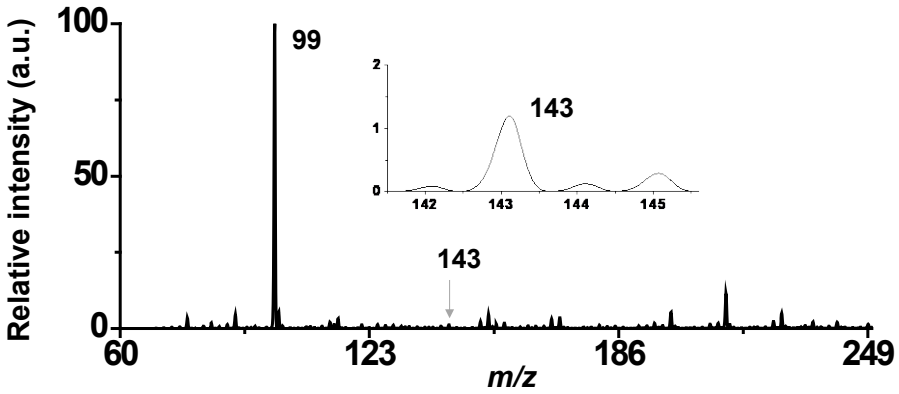

Figure S30. ESI MS spectrum of spray deposited sample after methanol extraction, showing low-intensity product peak. Inset displays a zoomed-in mass spec of the selected mass range showing the peak at *m/z* 143. This is due to the thermal decomposition of the product during extraction.

References

[1] J.-D. Chai, M. Head-Gordon, *Phys. Chem. Chem. Phys.* **2008**, *10*, 6615–6620.

[2] M. J. Frisch, G. W. Trucks, H. B. Schlegel, G. E. Scuseria, M. A. Robb, J. R. Cheeseman, G. Scalmani, V. Barone, G. A. Petersson, H. Nakatsuji, Gaussian 16, Revision C. 01. Gaussian, Inc., Wallingford CT. **2016**.

[3] A. V Marenich, C. J. Cramer, D. G. Truhlar, *J. Phys. Chem. B* **2009**, *113*, 6378–6396.

…

Author Contributions

P.B. planned the experiments. P.B., S.M., K.U., and B.K.S. helped in performing the experiments. K.S.S.V.P.R. and Y.S.S.R.K.C. helped with DFT calculations. The first draft of the manuscript was written by P.B. and it was finalized with the help of all the authors. The project was conceived under the guidance of T.P.